

## Lecture 8 : Examples of Compton Scattering

### 8.1 INTRODUCTION

Compton scattering is an important process and there are many examples of it in astrophysics. We will look at three here; the possible reheating of the Universe after the recombination era, X-ray emission from the radio lobes of double-source radio galaxies, and the high energy emission from the Crab nebula.

### 8.2 REHEATING OF THE UNIVERSE

After the so-called **recombination** of electrons and protons about 300,000 years after the Big Bang, the Universe changed from being **opaque** to being **transparent** to photons.

The temperature at this time was about 3000 K. The photons from that era are now seen, greatly red-shifted, as the 2.7 K microwave background radiation.

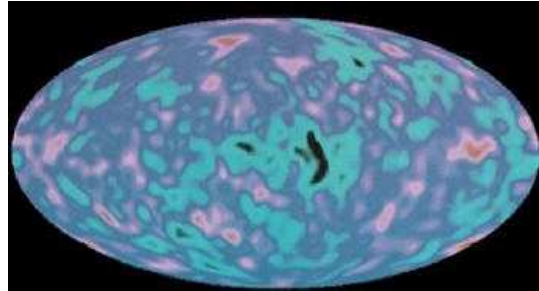
In the recombination, protons and electrons combined to form neutral Hydrogen, Helium and trace quantities of the other light elements. At this point, baryonic matter in the Universe consisted of about 75% Hydrogen and 25% Helium (by mass), with some small amounts of heavy elements (elements starting from Lithium). The distribution of this material was very close to, but not quite, uniform. These slight over- and under-densities were observed for the first time by the COBE satellite (launched in 1989) and amount to only a few parts in 100,000. The variations were mapped out over the whole sky, shown in figure 8.1, where the variations have been mapped on scales of greater than about 7 degrees, and since COBE for small parts of the sky at a resolution of a fraction of a degree.

After recombination, the Universe entered a period called the "Dark Ages", until gravitational attraction had operated on very slight over-densities in the matter distribution, leading to the formation of light emitting stars and galaxies. The Universe was optically observable again!

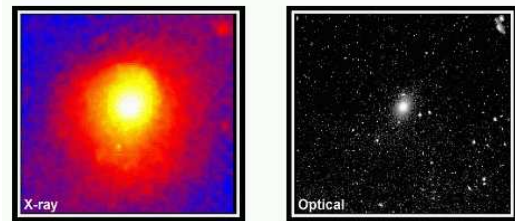
The process of star and galaxy formation led to some of the material in the Universe being heated to high temperatures, of order  $10^6-7$  K. This material is seen in X-ray observations of galaxy clusters, and is an important tracer of the mass distribution in these clusters. An example, the nearby Virgo cluster, is shown in figure 8.2.

Figure 8.3 shows the evolution of the temperature of the background photons from the recombination era to the present time.

What fraction of the Universe was re-heated by the processes of star and galaxy formation? We can place very strict limits on the amount because the microwave background spectrum is so very close to that of a black body distribution. Background photons passing through hot gas clouds on their way to us would be inverse-Compton scattered to higher wavelengths by the electrons in the clouds, and the black body spectrum slightly altered.



**Figure 8.1.** Map of the microwave background from the COBE mission. Source: <http://www.seas.columbia.edu/~h297/unesa/universe/universe-chapter5.html> Encyclopedia of Applied Physics, Vol. 23 (Page 47 - 81), 1998 WILEY-VCH Verlag GmbH, ISBN: 3-527-29476-7



**Figure 8.2.** Images of the Virgo cluster, in the optical (right) and in X-rays (left). The optical image shows the member galaxies, while the X-ray image shows the distribution of the hot gas in which the galaxies are embedded. Source : [http://imagine.gsfc.nasa.gov/docs/features/\\_topics/clusters\\_group/virgo\\_rosat.html](http://imagine.gsfc.nasa.gov/docs/features/_topics/clusters_group/virgo_rosat.html)

The change  $\Delta u_\nu$  in the black body spectrum  $u_\nu$  for a low number of scatterings is given by

$$\frac{\Delta u_\nu}{u_\nu} = y \frac{x e^x}{e^x - 1} \left( x \frac{e^x + 1}{e^x - 1} - 4 \right) \quad (8.1)$$

where  $y$  is the Compton parameter and  $x = h\nu/kT$ . For a low number of scatterings,  $y \ll 1$ . A mildly Comptonised black body spectrum, for  $y = 0.2$ , is shown in figure 8.4.

The COBE mission measured a background spectrum which is very close to black body, allowing strict limits on the amount of reheated gas that can have been produced since recombination:  $y \leq 10^{-3}$ . This result applies over large scales (more than of order 10 degrees). Later we will look at the very small amount of Comptonisation seen in the cosmic microwave background passing through well studied and nearby X-ray clusters. This Comptonisation is called the Sunyaev-Zel'dovich (or S-Z) effect. The S-Z effect is a means to measure distances to galaxy clusters directly, although it is technically quite difficult in practice.

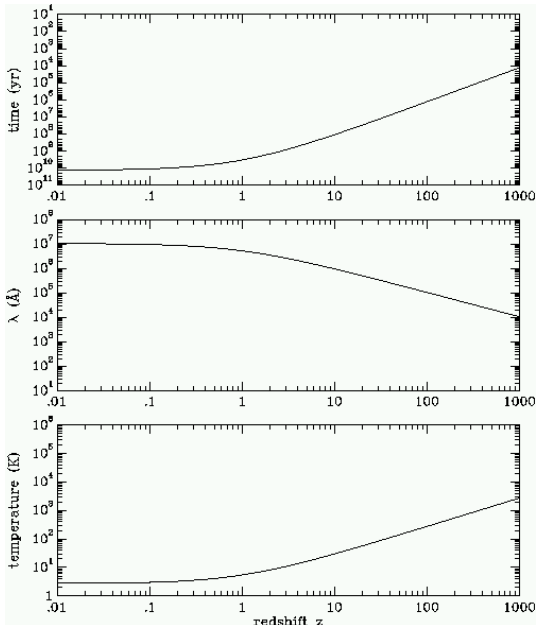


**Figure 8.3.** Change in the temperature and position of the peak wavelength of the black body background photons as a function of redshift. The time after the Big Bang is shown as a function of redshift in the top panel.

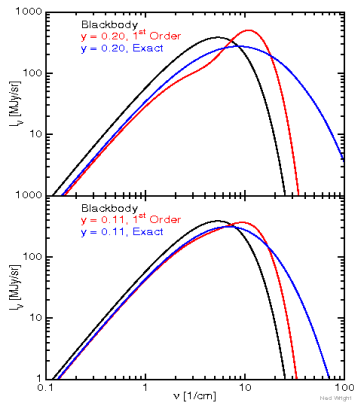


**Figure 8.4.** Comptonised black body spectrum. Original spectrum (solid line) and comptonised spectra for  $y=0.1$  and  $y=0.2$ . In each case, the 1st order approximation is shown in red, and an exact solution in blue. For the case  $y=0.2$ , the differences are already quite significant even in the R-J part of the spectrum, whereas for  $y=0.1$  the major difference is in the Wien part of the spectrum. More detailed information on computation of the Sunyaev-Zeldovich spectrum can be found here. Image courtesy of Ned Wright.

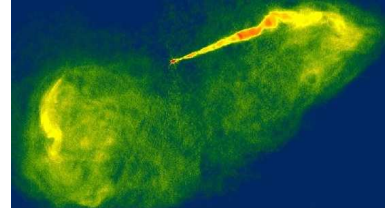


**Figure 8.5.** Radio image of NGC 9943, showing the two radio lobes, a jet and the central source (which is embedded in a host galaxy which is quite small on this scale). Source: Hubble Space Telescope.

### 8.3 INVERSE COMPTON X-RAYS FROM RADIO LOBES

A more interesting example of comptonisation is when cosmic background photons pass through the lobes seen around radio galaxies. These lobes contain highly relativistic electrons, which can boost the wavelength of the source photons dramatically.

Many radio galaxies show two sources of emission on either side of a central galaxy, with one or both of these “lobes” connected to a central bright source by thin jets. The “engine” powering these jets is thought to be a massive black hole at the center of the host galaxy. The jets and lobes can be remarkably distant from the black hole, up to Mpc (our on Galaxy is a fraction of this size with a diameter of order 40 kpc).

At radio wavelengths double radio sources are amongst the brightest known. A typical source may contain  $10^{61}$  ergs in energy content, equivalent to some  $10^{10}$  supernovæ.

The lobes are typically dominated by synchrotron emission, indicating the presence of magnetic fields and relativistic electrons. Typical values are magnetic field strengths of a few  $\mu\text{Gauss}$  and lorentz factors for the electrons of  $\gamma \approx 10^3 - 10^5$ .

$$\nu = \gamma^2 \nu_0. \quad (8.2)$$

The frequency of the photons depends on redshift, so for lobes around a galaxy of redshift  $z$ , the frequency of the source photons is

$$\nu_0 \approx 10^{11}(1+z)\text{Hz}. \quad (8.3)$$

The boosted photons can have frequencies  $\nu$  of order  $(10^6 - 10^{10}) \times 10^{11}$  Hz, putting them in the X- or  $\gamma$ -ray region.

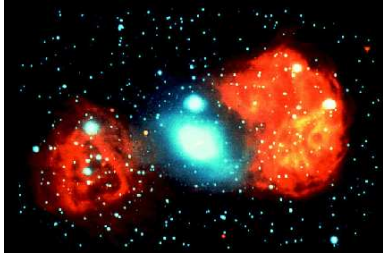
Cosmic background photons passing through the cloud can be comptonised, with frequency boosting of order  $\gamma^2$ ,

Such X-rays have been observed in the nearby radio galaxy Fornax A (Harris et al 1994, Kaneda et al 1995) using ROSAT (the Röntgen Satellit, a German/British X-ray observatory) and ASCA (Advanced Satellite for Cosmology and Astrophysics, which is Japanese built).

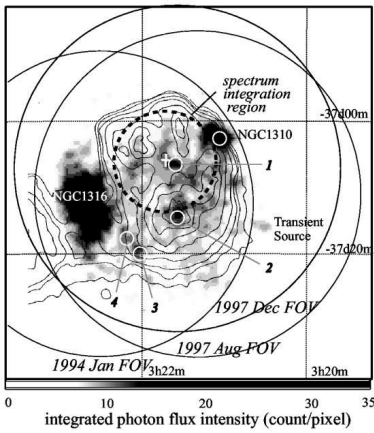
#### 8.3.1 Case study : Fornax A

Figure 8.6 shows the galaxy Fornax A, or NGC 1316, in a combined image in optical and radio wavelengths.

The galaxy has two prominent lobes of emission in the radio, which have been observed to be also a source of in



**Figure 8.6.** Optical and radio images of the galaxy Fornax A, or NGC 1316. Source: <http://www.astronica.org/Gallery/vla2/vla2-21.html>



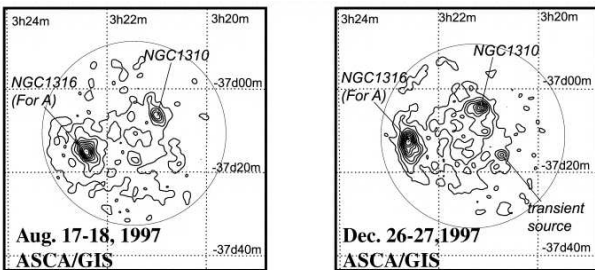
**Figure 8.7.** Combined optical and radio image of Fornax A, with the region observed by ASCA in X-rays marked by the heavy dashed circle. Source: Tashiro et. al. 2000.

X-rays; the interpretation is that these X-rays are inverse-Comptonised radio photons.

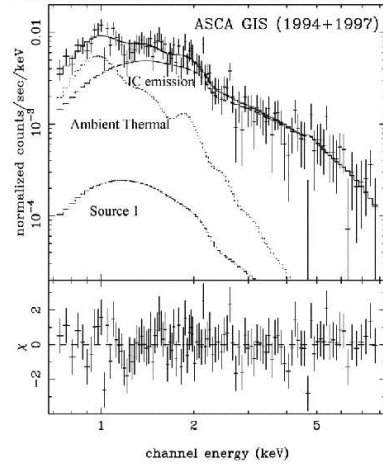
Recently, the western lobe has been observed with the ASCA satellite (Tashiro, et al 2000, ApJ, 546, L19). An image of the region examined is shown in figure 8.7 as a heavy dashed circle. As can be seen, there are a number of background sources which must be dealt with carefully.

Figure 8.8 shows the ASCA image of this whole region. General X-ray emission is seen in the area of the western lobe.

A spectrum of the X-ray emission in the western lobe is shown in Fig 8.9. The spectrum is roughly a power law



**Figure 8.8.** Two X-ray images of the western lobe of Fornax A, taken with ASCA.



**Figure 8.9.** Spectrum of the X-ray emission from the western lobe of Fornax A, with a model fit based on inverse-Comptonisation microwave background photons (marked “IC emission”).

with a slope of  $0.7 \pm 0.1$ , which is very similar to the slope of the radio emission from this region ( $0.9 \pm 0.2$ ), (i.e. the synchrotron emission from the relativistic electrons in the cloud). These two power laws have similar slope, indicating that they are produced by the same (power law) distribution of electrons.

The cloud is producing its own synchrotron (radio) photons, but an analysis indicates that there are many more background photons passing through the cloud than locally produced photons. Hence, the X-ray emission is probably dominated by inverse-Comptonised background photons, rather than self-Comptonisation of the synchrotron photons.

#### 8.4 SUNYAEV-ZEL'DOVICH EFFECT

As discussed in section 8.2 and shown in Fig 8.4, Cosmic background photons can be slightly Comptonised if they pass through a region of 2hot electrons. Although the effect is very weak, it can be used to measure the distances to clusters of galaxies, making it a very interesting cosmological probe. Unfortunately it is technically quite difficult, and it is not yet competitive with other distance determination methods, although it may be in the future.

The photons are slightly Comptonised by passing through a medium of hot electrons (with energies typically in the X-ray region). In such a case one may use a simplified form of the Kompaneets Equation:

$$\frac{\partial n}{\partial y} = \frac{1}{x^2} \frac{\partial}{\partial x} \left( x^4 \frac{\partial n}{\partial x} \right). \quad (8.4)$$

**Problem 8.1** For thermal photons with occupation  $n(x) = (e^x - 1)^{-1}$  (where  $x = h\nu/kT$ ), show that

$$\frac{\partial n}{\partial y} = \frac{x e^x}{(e^x - 1)^2} \left[ \frac{x(e^x + 1)}{(e^x - 1)} - 4 \right]. \quad (8.5)$$

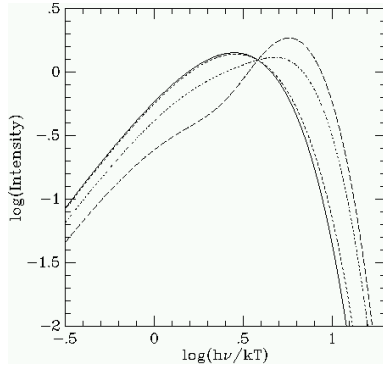


**Figure 8.10.** Slightly comptonised black body spectrum for various values of the  $y$  parameter. The Planck spectrum is shown as a solid line, with three spectra showing from top to bottom (in the Raleigh-Jeans regime), the S-Z effect for  $y = 0.01, 0.1$  and  $0.2$ . All spectra pass through the same cross-over frequency of  $h\nu = kT \approx 3.83$ .

The radiation is very weakly scattered, so that the occupation state of the photons is very close to the Planck state

$$n(x) = (e^x - 1)^{-1}. \quad (8.6)$$

By integrating along the path length taken by photons through the cluster, we have a change  $\Delta I$  in the intensity  $I = i_0 x^3 n(x)$  of the radiation

$$\Delta I = i_0 y g(x) \quad (8.7)$$

where

$$i_0 = 2 \frac{kT_0^3}{h^2 c^2} \quad (8.8)$$

and  $T_0$  is the temperature of the Cosmic background photons at the cluster (see Fig 8.3), and

$$g(x) = \frac{x^4 e^x}{(e^x - 1)^2} \left[ x \frac{e^x + 1}{e^x - 1} - 4 \right]. \quad (8.9)$$

Figure 8.4 shows the effect on the Planck spectrum for a relatively large compton factor of  $y = 0.2$ . The intensity difference between the uncomptonised and comptonised spectra is zero at a point called the **cross-over frequency**.

**Problem 8.2** Show that the cross-over frequency occurs at  $x = h\nu/kT \approx 3.83$ .

The cross-over frequency is independent of  $y$ , as illustrated in Fig 8.10.

**Problem 8.3** Show that the cross-over frequency for the microwave background is at approximately 217 GHz.

The compton  $y$ -parameter is defined as

$$\int \frac{kT_e}{m_e c^2} n_e \sigma_T dl \quad (8.10)$$

along a path  $l$  through the gas cloud, so that we may also write the time derivative of the occupation function  $n(x)$  as

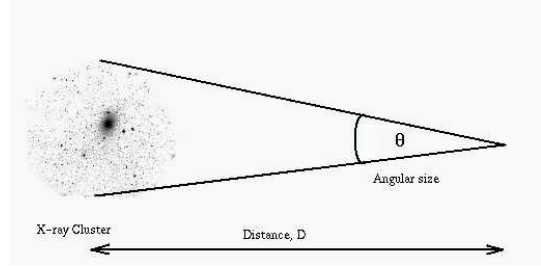


**Figure 8.11.** Schematic of Sunyaev-Zel'dovich effect for a cluster of galaxies embedded in a hot X-ray emitting plasma.

$$\frac{\partial n}{\partial t} = \frac{kT_e}{m_e c} \frac{\sigma_T n_e}{x^2} \frac{\partial}{\partial x} \left( x^4 \frac{\partial n}{\partial x} \right) \quad (8.11)$$

where  $T_e$  is the electron temperature and  $n_e$  is the electron density.

The temperature change  $\Delta T$  induced by passage through the plasma is

$$\Delta T = y \left[ x \frac{e^x + 1}{e^x - 1} - 4 \right] T_0 \quad (8.12)$$

and so in the Raleigh-Jeans (R-J) regime ( $x \ll 1$ ), we have

$$\frac{\Delta I}{I_0} = \frac{\Delta T}{T_0} = -2 \left( 1 + \frac{x}{2} \right) y. \quad (8.13)$$

Note that this equation assumes no change in the properties of the cluster (e.g. the potential or gas temperature) as a result of the comptonised photons. This is a very good approximation for the case considered here.

Eqn 8.13 gives us a first estimate of the Sunyaev-Zel'dovich effect in terms of a temperature difference or intensity difference for radiation passing through the cluster (relative to, say, radiation passing by the edge of the cluster). There are plenty of further effects one can take into account when computing the magnitude of this effect, such as the motion of the cluster through space (relative to the general expansion of the Universe). Both the transverse velocity of the cluster on the sky and the velocity along the line-of-sight introduce very small corrections to the effect. Further, the gravitational field of the cluster can act like a gravitational lens, slightly magnifying the intensity of the background photons. For typical clusters, these extra effects are very small.

## 8.5 OBSERVING THE S-Z EFFECT

Detection of the S-Z effect observationally is very interesting because

- it shows that there are cosmic background photons passing through the source, i.e. the background radiation is a cosmic phenomenon,
- it is independent of the cluster redshift, which is a highly desirable and unusual property, and permits a measurement of the distance of the cluster.

Consider a cluster of galaxies at some distance,  $D$ , with angular size  $\theta$ . Let us model the density profile  $n_e$  of the electrons in the ionised gas by a simple function,

$$n_e(r) = n_0 \left(1 + \frac{r^2}{r_c^2}\right)^{-3\beta/2} \quad (8.14)$$

where  $r$  is radius,  $r_c$  is a core radius,  $n_0$  is the central density and  $\beta$  is a power law index. Let us assume that the temperature of the plasma  $T_e$  is constant as a function of radius. The current generation of X-ray satellites will allow the temperature profile of the plasma in X-ray clusters to be determined, so that in the past one has had to make this assumption to keep things simple.

The plasma emits thermal bremsstrahlung, with a flux  $e_{\text{ff}}$ ,

$$e_{\text{ff}} = 1.4 \times 10^{-27} T_e^{0.5} n_e n_i Z^2 g_{\text{BB}} \quad (8.15)$$

while the temperature difference  $\Delta T_0$  of the microwave background coming through the cluster is given by

$$\frac{\Delta T_0}{T_0} = -2 \left(1 + \frac{1}{2} \frac{h\nu}{kT_0}\right) \int \sigma_T n_e dl \quad (8.16)$$

The quantity  $\frac{\Delta T_0}{T_0}$  can be measured in the radio region (i.e. the R-J part of the microwave background).

Eqns 8.15 and 8.16 allow us to derive the electron density in the cluster, since the temperature  $T_e$  of the electrons can be established independently from lines in the spectrum or the thermal cutoff in the X-ray spectrum. One can thus derive the cluster size,  $r_c$ .

The cluster size (or core radius) is a function of redshift,  $z$  in an adopted cosmological model:

$$r_c \propto \frac{zq_0 + (q_0 - 1)[(1 + 2zq_0)^{0.5} - 1]}{H_0 q_0 (1 + z^2)} \quad (8.17)$$

where  $H_0$  is the Hubble constant and  $q_0$  is the deceleration parameter. For low redshift sources, this allows a measurement of the expansion rate of the Universe  $H_0$  and for high redshift sources  $H_0$  and  $q_0$  can be mapped out.

### 8.5.1 Measurements

Since the temperature difference between the middle of a cluster and the edge is so small, a differential technique is used, switching the beam of the telescope rapidly between the cluster center and a reference field. Note that in the R-J region, the temperature difference is essentially independent of the frequency  $\nu$ . Measurements have been made with the NRAO 11 meter, the Ryle telescope ( $8 \times 13$  meter dishes), the 100 meter Bonn telescope and the 40 meter OVRO telescope.

About half a dozen clusters have been measured, and they yield a Hubble constant of order

$$H_0 = 50 \pm 10 \text{ km s}^{-1} \text{ Mpc}^{-1}. \quad (8.18)$$

With increasingly sensitive X-ray satellites, which will allow the temperature profile in the cluster to be reconstructed  $T_e(r)$ , as well as detailed surface density measurements of the X-ray flux ( $e_{\text{ff}}(r)$ ), this may provide an independent means of determining the cosmological parameters for the future.

Simulations of deep X-ray/Radio comptonised microwave background maps show strong dependence on the cosmological density parameter  $\Omega$  and the distribution function of cluster mass. These effects may be measurable in the next generation of instruments.